Duchenne muscular dystrophy is driven by defective membrane repair and annexin-A2 dysregulation in skeletal muscle

Mégane Le Quang[1,2,7*], Léna d'Agata[1*], Phoebe Rassinoux[1,3], Joana Ruiz[1], Céline Gounou[1], Antoine Salesses[1], Flora Bouvet[1], Kamel Mamchaoui[4], Sandra Dovero[5], Guilhem Solé[6], Marie-Laure Martin-Négrier[2,6,7] and Anthony Bouter[1**]

[1]Univ. Bordeaux, CNRS, Bordeaux INP, CBMN, UMR 5248, F-33600 Pessac, France.

[2]Department of Pathology, University Hospital (CHU) of Bordeaux, Pellegrin Hospital, Place Amélie Raba Léon, 33000, Bordeaux, France.

[3]present address: Institut NeuroMyogène (INMG) - Laboratoire Physiopathologie et Génétique du Neurone et du Muscle, Université Claude Bernard Lyon 1, CNRS UMR 5261, INSERM U1315, Lyon, France.

[4]Sorbonne Université, Inserm, Institut de Myologie, Centre de Recherche en Myologie, F-75013, Paris, France.

[5]Univ. Bordeaux, CNRS, HistoCARE Facility, IMN, UMR 5293, Bordeaux, France.

[6]Centre de Référence des Maladies Neuromusculaires AOC, Service de Neurologie et Maladies Neuromusculaires, FILNEMUS, EURONMD, Hôpital Pellegrin, CHU de Bordeaux, France.

[7]Univ. Bordeaux, CNRS, IMN, UMR 5293, Bordeaux, France.

*Contribute equally to this work

**Corresponding author, e-mail: anthony.bouter@u-bordeaux.fr; phone: +33 540006860

Running title: Membrane repair and annexins in DMD

ABSTRACT

Background:

Duchenne muscular dystrophy (DMD) is caused by mutations in the *DMD* gene, which encodes dystrophin in skeletal muscle cells. Although the role of dystrophin as a structural protein is well known, the cellular processes underlying myofiber degeneration are still not fully understood. Despite advances from studies in murine models, these models do not fully replicate the human pathology.

Methods:

We investigated sarcolemmal integrity, membrane repair capacity, and annexin protein expression in DMD patient muscle biopsies and human skeletal muscle cell lines using immunohistochemistry, a shear stress-based injury assay, western blotting, and live-cell imaging of GFP-tagged annexins.

Results:

We identified defective membrane repair in DMD skeletal muscle cells, independent of increased membrane fragility. Massive intracellular IgG uptake and impaired resealing after mechanical stress, respectively observed ex vivo and in vitro, confirmed this defect. We also observed altered expression patterns of annexins, a family of key proteins involved in membrane repair. Control skeletal muscle cells upregulate ANXA5 and ANXA6 upon mechanical stress, likely as part of an adaptive mechanism to counteract membrane damage. Conversely, DMD cells failed to induce this upregulation. Strikingly, ANXA2 was not only significantly overexpressed in DMD cells but also aberrantly localized to the extracellular space due to the defect in membrane repair. This extracellular ANXA2 is associated with adipocyte accumulation in muscle tissue, suggesting a mechanism similar to that seen in dysferlinopathies.

Conclusions:

Our findings propose that ANXA2 contributes to muscle degeneration in DMD and highlight it as a potential therapeutic target to prevent adipogenesis and muscle loss.

Keywords: Duchenne muscular dystrophy, membrane repair, annexin, ANXA2, skeletal muscle

Abreviation: ANXA2: Annexin-A2; DMD: Duchenne muscular dystrophy; FAP: fibro-adipogenic progenitors; IgG: immunoglobulin type G; MD: muscular dystrophies; PI: propidium iodide

1. Introduction

Skeletal muscle fibers are subjected to constant mechanical stress due to contraction, stretching, and shearing forces, which can result in transient disruptions of the sarcolemma [1]. Efficient membrane repair is essential to preserve myofiber viability, and defects in this process contribute to the progression of degenerative muscle diseases, including muscular dystrophies (MDs). Limb-girdle muscular dystrophy type 2B (LGMD2B), now classified as LGMDR2, is a prototypical example of a membrane repair disorder. Caused by mutations in the *DYSF* gene encoding dysferlin, LGMD2B is characterized by defective sarcolemmal resealing, leading to myofiber necrosis and muscle wasting [2]. Notably, annexin-A2 (ANXA2), a calcium-dependent phospholipid-binding protein involved in membrane repair, is upregulated in LGMD2B muscle possibly as a compensatory response to membrane fragility [3,4]. However, persistent sarcolemmal damage results in leakage of intracellular contents, triggering infiltration of fibro-adipogenic progenitors (FAPs) and macrophages [5]. In murine models, extracellular ANXA2 has been shown to promote adipogenic differentiation of FAPs, contributing to fatty replacement of muscle fibers [3].

Duchenne muscular dystrophy (DMD) is an X-linked disorder caused by mutations in the *DMD* gene, resulting in the loss of dystrophin, which is a structural protein that anchors the actin cytoskeleton to the extracellular matrix via the dystrophin-glycoprotein complex (DGC) [6,7]. Dystrophin deficiency destabilizes the sarcolemma, increasing susceptibility to damage during contraction and disrupting DGC-associated signaling pathways [8,9]. Moreover, disruptions in the DGC complex affect the distribution of associated proteins, further exacerbating the loss of muscle function [10]. Although sarcolemmal fragility in the *mdx* mouse model of DMD has been linked to impaired mitochondrial function and defective membrane repair [11], species-specific differences raise uncertainty about the relevance of these findings to human disease [12].

Here, we investigate membrane repair capacity in human DMD muscle using muscular biopsies and patient-derived skeletal muscle cell lines. We show that DMD myofibers exhibit defective membrane resealing, as evidenced *in vivo* by increased intracellular accumulation of IgG in myofibers with a necrotic outcome and impaired membrane integrity following mechanical stress *in vitro*. We further identify dysregulation of multiple annexins with ANXA2 significantly overexpressed and mislocalized to the extracellular space in DMD muscle. This pattern mirrors the annexin pathology observed in LGMD2B and correlates with adipocyte accumulation, implicating ANXA2 misregulation as a potential driver of fibro-adipogenic remodeling in DMD.

2. Methods

2.1. Patient Biopsies

Frozen muscle biopsies from 10 DMD patients with confirmed mutations were obtained from the bio-bank of Bordeaux University Hospital (COLMYONEU, Table S1 and S2). As a control, 10 frozen muscle biopsies performed for chronic muscle pain or weakness without characterized neuromuscular conditions, elevated creatine kinase levels and histopathological anomalies were used (Table S3). Informed consents have been obtained from all patients and the study was approved by the Ethics Committee of Bordeaux University Hospital (CER-BDX 2025-214).

2.2. Immortalized Patient-Derived Skeletal Muscle Cells

Human-derived skeletal muscle cell lines were obtained from the Center of myology (UMRS974, Paris, France). Healthy, LGMD2B and DMD patient-derived skeletal muscle cell lines were immortalized with CDK4 and Telomerase-expressing pBABE retroviral vectors as described previously [13]. The immortalized DMD muscle cell lines tested were AB1098 and 6594 [14], herein referred as to DMD1 and DMD2, respectively. Both DMD cell lines present deletions of DMD exons 48–50 leading to the absence of the expression of dystrophin [14,15]. The immortalized healthy muscle cell lines LHCN-M2 and KM1421 were used as controls, herein referred as to CTL1 and CTL2, respectively. We used also the LGMD2B muscle cell line 578 as a positive control, since LGMD2B is associated with a defect in membrane repair [2,13,16]. Cell culture media and reagents were from ThermoFisher Scientific (Waltham, MA, USA) except when otherwise stated. Myoblasts were cultured in a skeletal muscle medium composed by one volume of Medium 199 with glutaMAX™ (Gibco® by Thermo Fisher Scientific, Waltham, MA, USA), four volumes of Dubelcco's modified Eagle Medium (DMEM) with high-glucose and glutaMAX™ and without pyruvate (Gibco® by Thermo Fisher Scientific, Waltham, MA, USA) supplemented with 20% fetal bovine serum, 50-µg/mL gentamycin and a commercial mix of skeletal muscle cell growth medium supplements (ref. C-39365, Promocell, Heidelberg, Germany), which included 12.5-g/mL fetuin, 2.5-ng/mL human recombinant epidermal growth factor, 0.25-ng/mL basic fibroblast growth factor, 2.5-µg/mL insulin, 0.1-µg/mL dexamethasone. The 24h-differentiated myoblasts and myotubes were obtained by cultivating 90%-confluence myoblasts respectively for one and three days in a differentiation medium, composed of the skeletal muscle medium supplemented only with 10µg/mL insulin.

2.3. Muscle Shear Stress Assay

Experiments were performed as previously described [17]. Differentiated myoblasts for 24 hours, at a concentration of 5×10^5 per mL, were divided into two populations: the stressed population was passed ten times through a 30G needle, while the untreated population remained in resting conditions and served as a control. To assess membrane repair, 50 µL of each population were incubated with a mixture of Hoechst (20 µg/mL, Sigma-Aldrich) and PI (2 µg/mL, Sigma-Aldrich). PI-positive (damaged) and Hoechst-positive (total) cells were counted by fluorescence microscopy (IX81, Olympus).

2.4. Effect of Shear Stress on Survival Rate and ANX Expression

To assess survival rate, cells were seeded in growth conditions after submitted to the muscle shear stress assay and counted 24 hours later. The survival rate was calculated as the ratio of living cells at 24h to number of seeded cells. To overcome mortality related to experimental conditions (room temperature and atmospheric CO_2), common to both the unstressed and stressed populations, live cell concentration within the untreated population 24 hours after the experiment was measured and the mortality rate due to experimental conditions was calculated. This correction factor was applied to cells subjected to shear stress. Secondly, a significant loss of 10-20% of cell suspension was observed during the shear stress treatment, mainly due to dead volume in the needle-syringe system. To eliminate this bias, the volume of cell suspension seeded after shear stress was systematically measured and all data were proportionally corrected for this loss. We then determined the survival rate by calculating the ratio of the number of surviving cells in the stressed condition to the number of surviving cells in resting condition. The impact of mechanical stress on ANX expression was analyzed by western blot, by comparing expression between stressed and non-stressed cells 24 hours after shear stress.

2.5. Immunohistochemical Analysis of Muscle Sections

Immunofluorescence was performed on 8-µm frozen cross-sections. Blocking was done with 3% BSA and 3% NGS. Primary and secondary antibodies were incubated with NGS 3% respectively at 4°C overnight and at room temperature 2 h. The following primary antibodies were used: rabbit polyclonal anti-ANXA1 (1:100, Boster, PA1006), mouse monoclonal anti-ANXA2 (1:1000, Sigma-Aldrich, WH0000302M1), mouse monoclonal anti-ANXA5 (1:500, Abcam, AB54775), mouse monoclonal anti-ANXA6 (1:500, Santa Cruz, sc-271859), mouse monoclonal anti-MHCf (1:100, Novocastra, WB-MHCf), mouse monoclonal anti-perilipin (1:100, Santa-Cruz, sc-390169) and rabbit polyclonal anti-IgG conjugate with FITC (1:50, Dako Agilent, F0202). Co-labeling with rat monoclonal anti-Laminin α-2

(1:1000, Santa Cruz, sc-59854) or rabbit polyclonal anti-Laminin (1:1000, ThermoFisher, PA116730) was made. Staining was visualized using relevant secondary antibodies conjugated to AlexaFluor 488 or 568 (1:500, Invitrogen). Nuclear counterstaining was performed with Hoescht 33342 (Sigma-Aldrich). All slides were digitized using a high-resolution slide scanner (Panoramic Scan II, 3DHISTECH Ltd, France) at x20 magnification. Quantification of the biopsies was performed using ImageJ software. The IgG-positive area was calculated by applying thresholding to exclude non-specific staining and by measuring the total positive area (excluding any epi- or perimysium staining) relative to the entire muscle cross-section. The number of positive fibers was determined by thresholding the image to exclude non-specific staining.

2.6. Western Blot

For muscle cell lines, 2×10^6 cells were trypsinized, pelleted and re-suspended in 300 µL of D-PBS supplemented with 1 mM EGTA. Protein extracts were obtained by sonicating ice-cold cell suspension with a Branson digital sonifier (amplitude 20%, duration 2 min, interval 5 s and pulse 5 s). Two successive centrifugations at 8,000g for 1 min allowed to remove cell debris. 10 µg protein extracts, together with the Precision Plus Protein Dual Color Standards (Bio-Rad, Hercules, CA, USA) were separated on a 10% SDS-PAGE. Transfer onto PVDF membrane was performed for 1 h at 100 V. GAPDH was detected with a rabbit anti-GAPDH polyclonal antibody (Santa Cruz Biotechnology) diluted 1:20000, as a loading control. Revelation was performed using secondary antibodies conjugated to horse-radish peroxidase (GE-Healthcare, Chicago, IL, USA) diluted 1:2000 in saturation solution and Opti-4CN™ colorimetric kit (Bio-Rad, Hercules, CA, USA).

For biopsy analysis, 8-µm frozen sections were homogenized with a lysis buffer containing 2% glycerol, 2% SDS, and Tris/HCL pH 6.4 (0,125 mol/L) during 30 min before sonication for 10 min in ice-cold cell suspension. Lysates were stored at -20°C and used within a week. Protein concentration was measured using BCA assessment (BCA1, Sigma-Aldrich). Western blots were performed with 10-20 µg protein extracts separated on SDS-PAGE using stain-free 10% acrylamide gel (Biorad, TGX Stain-Free™ FastCast™ Acrylamide Kit, 10%). Electrophoretic transfer was performed with the Trans-Blot Turbo Transfer System (BioRad) during 7 min at 1.3A/25V. Total protein signals were measured using the Chemi-Doc imager (Bio-Rad) and ImageLab software. Revelation was performed by chemiluminescence using secondary antibodies conjugated to horse-radish peroxidase (GE-Healthcare, Chicago, IL, USA) diluted 1:2000 in saturation solution and Clarity™ Western ECL substrate (Bio-Rad). Annexins were detected with the same antibodies as for immunofluorescence diluted 1:1000 in saturation solution composed by Tris buffer saline (10-mM Tris, 150-mM NaCl, pH 8.0)

supplemented with 0.1% Tween20 and 5% non-fat dry milk. ImageLab software was used to measure the relative intensity of protein bands.

2.7. Subcellular Trafficking of ANXA2 Fused to Fluorescent Proteins in Damaged Skeletal Muscle Cells

Sketelal muscle cells expressing the ANXA2-GFP fusion protein were obtained as previously described [18]. Membrane damage was performed on myoblasts differentiated 24h by laser ablation, as previously described [17]. Briefly, myoblasts were cultured and differentiated in a 35-mm glass bottom dish equipped with a square-patterned coverslip (MatTek, Ashland, MA, USA). To induce membrane damage, cells were irradiated at 820 nm with a tunable pulsed depletion laser Mai Tai HP (Spectra Physics, Irvine, USA) of an upright two-photon confocal scanning microscope (TCS SP5, Leica, Wetzlar, Germany) equipped with an HCX APO L U-V-I 63.0 0.90 water lens. Irradiation consisted of 1 scan (1.3 s) of a 1 µm x 1 µm area with a power of 110 (± 5) mW. Images of 512 x 512 were acquired at 1.3 s intervals with pinhole set to 1 Airy unit. At least three independent experiments were performed for each cell type.

2.8. Statistics

Data are presented as mean values (±SEM) from at least three independent experiments performed in triplicate. The statistical significance of data was assessed by a Mann–Whitney or Wilcoxon test, as indicated in the legend of Figures. A probability value less than 0.05 is used for statistical significance. *$p < 0.05$, **$p < 0.01$, ***$p < 0.001$, ****$p < 0.0001$.

3. Results

3.1. Human DMD Muscle Cells Suffer from a Defect in Membrane Repair

To assess whether membrane repair is impaired in DMD skeletal muscle cells, we analyzed sarcolemmal integrity in patient biopsies using immunostaining for intracellular IgG uptake, a well-established marker of membrane permeability [19]. Compared to control, DMD muscle exhibited extensive IgG accumulation both within the interstitial space and intracellularly in a substantial proportion of myofibers (**Figure 1A–C**). This indicates widespread membrane damage and the consequent entry of serum IgG into muscle fibers due to loss of membrane integrity, likely resulting from chronic and repeated mechanical stress. Notably, IgG labeling within DMD biopsies was spatially heterogeneous, with discrete regions displaying high or low signal intensity (**Figure S1**), suggesting local variation in mechanical vulnerability or disease progression. Collectively, these findings demonstrate frequent and regionally variable disruption of membrane integrity in DMD skeletal muscle. To investigate whether DMD skeletal muscle cells exhibit defective membrane repair, we subjected two patient-derived skeletal muscle cell lines to a recently established shear stress assay [17]. This assay involves passing 24-hour–differentiated myoblasts through a fine-gauge needle, inducing mechanical membrane disruption.

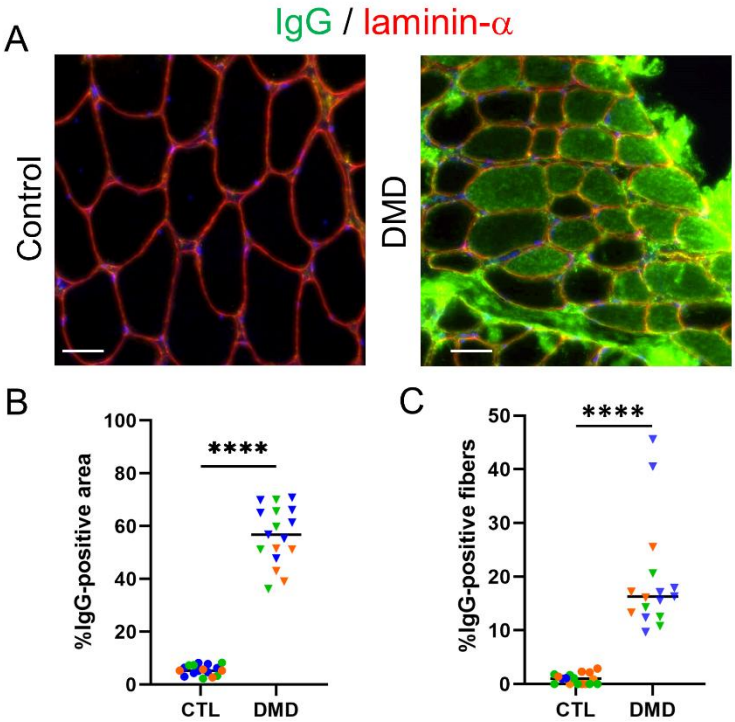

FIGURE 1 Impaired sarcolemma integrity in patients with DMD. A) Sarcolemma integrity was assessed by IgG staining (green) in skeletal muscle samples from control and DMD patients. Co-staining of laminin (red, basal lamina) and Hoechst (blue, nucleus) was also performed. Scale bar = 20 µm. B-C) The percentage of area with IgG positivity (B) and IgG-positive fibers (C) was calculated for control (circles, n=3) and DMD patients (inverted triangles, n=3). Each color corresponds to a control individual or a patient. Mann-Whitney test. ****$p < 0.0001$.

We previously demonstrated that at this stage of differentiation, healthy myoblasts possess a functional, Ca^{2+}-dependent membrane repair machinery capable of resealing shear-induced damage [17]. DMD myoblasts were analyzed alongside two control cell lines and a positive pathological control cell line derived from a patient with LGMD2B, a dystrophy caused by impaired membrane repair [2]. In the presence of extracellular Ca^{2+}, control cells showed low levels of unrepaired membrane damage - 2.5 ± 1.8% (CTL1) and 2.7 ± 0.9% (CTL2) (**Figure 2B**). By contrast, LGMD2B myoblasts exhibited a significantly higher rate of damage (8.2 ± 2.1%), consistent with a known repair defect (**Figure 2B**). DMD myoblasts displayed similarly elevated levels of unrepaired membrane disruption - 8.1 ± 2.1% (DMD1) and 6.4 ± 1.1% (DMD2) - suggesting a comparable defect in membrane resealing. Because dystrophin is essential for maintaining sarcolemmal stability, the increased damage observed in DMD cells could reflect either defective repair or heightened membrane fragility. To distinguish between both possibilities, we repeated the assay in the absence of Ca^{2+}, a condition that abolishes repair,

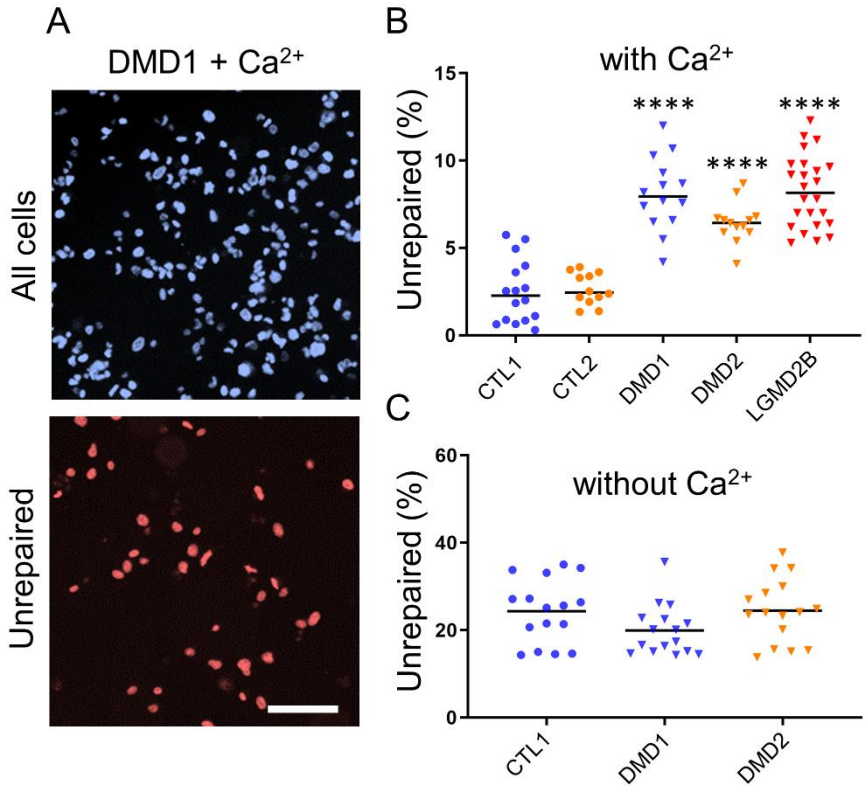

FIGURE 2 Identification of defective membrane repair process in human DMD muscle cells. A) Control, DMD and LGMD2B cell lines were subjected to the muscle shear stress assay [17] and propidium iodide (PI, red) permeability assay was performed to quantify unrepaired cells. Hoechst was used to stain all the cells (blue). Example of images acquired for DMD1 cells submitted to the shear stress muscle assay in the presence of Ca^{2+}. B-C) Scatter plots with the mean value representing PI-positive cells when the shear stress assay was performed in the absence (C) or the presence of 2mM Ca^{2+} (B) for control (blue circles, n = 16), DMD (inverted triangle, n = 16), and LGMD2B (red inverted triangle, n = 24). Mann-Whitney test using CTL1 cells as a reference. **** $p < 0.0001$.

allowing assessment of intrinsic membrane susceptibility to shear-induced rupture. Under these conditions, both control and DMD cells exhibited about 20% membrane disruption with no significant difference (**Figure 2C**), indicating comparable baseline fragility. Together, these findings demonstrate that the elevated level of unrepaired cells observed in DMD myoblasts under permissive (Ca^{2+}) conditions results from impaired membrane repair capacity rather than increased membrane fragility.

To further assess the functional consequences of impaired membrane repair in DMD cells, we evaluated cell survival 24 hours after exposure to mechanical injury. Control and DMD 24-hour–differentiated myoblasts were subjected to the shear stress assay and subsequently replated in growth medium. After 24 hours, cell viability was quantified. Cell survival following mechanical stress was quantified by comparing the number of viable cells 24 hours post-shear stress to untreated controls. Control myoblasts exhibited near-complete survival, indicating that shear stress did not compromise long-term viability in cells with intact membrane repair capacity (**Figure S2**). In contrast, DMD-derived myoblasts showed significantly reduced survival rates, at respectively 59.6 ± 18.3% (DMD1) and 60.7 ± 14.0% (DMD2), demonstrating that mechanical stress induces substantial cell death in the absence of efficient membrane repair. Interestingly, the observed mortality rates exceeded the proportion of unrepaired cells detected immediately after shear stress (**see Figure 2**), suggesting that some cells, although initially capable of resealing, may have incurred sublethal damage that compromised survival over time. Alternatively, delayed cell death may occur in cells that withstood initial membrane rupture but failed to recover from mechanical injury. Together, these findings support the conclusion that defective membrane repair in DMD myoblasts leads to delayed cell death following mechanical challenge. *In vivo*, such a defect likely contributes to progressive muscle fiber necrosis and the pathological release of intracellular components into the extracellular space.

3.2. Annexin Expression is Dysregulated in DMD Muscle Cells

In LGMD2B, impaired membrane repair is accompanied by dysregulation of annexin family members, notably ANXA1 and ANXA2, which may exacerbate disease progression by interfering with repair pathways or amplifying inflammatory signaling [4,20–22]. To investigate whether a similar pattern occurs in DMD, we analyzed the expression of ANXA1, ANXA2, ANXA5, and ANXA6, which are key components of the membrane repair machinery, by western blotting in both human skeletal muscle cell lines and patient biopsies. We first compared annexin expression profiles in muscle biopsies from control individuals and DMD patients (**Figure 3A**). As expected, western blot analysis revealed single bands corresponding to the predicted molecular weights of ANXA1 (37 kDa), ANXA2 (36 kDa), ANXA5 (35 kDa), and ANXA6 (68 kDa) (**Figure 3A**). Previous studies in dysferlin-deficient mice have identified a

truncated ANXA6 isoform that impairs membrane localization of the full-length protein [23,24]. Despite extensive efforts, we did not detect any truncated ANXA6 species in human control or DMD muscle biopsies (**Figure 3A and Figure S3**), suggesting that this isoform may be specific to murine and/or dysferlinopathic skeletal muscle. Quantitative analysis showed that ANXA5 levels were comparable between DMD and control biopsies (**Figure 3B**). ANXA6 expression was moderately but significantly elevated in DMD samples, with an average twofold increase. In contrast, ANXA1 and ANXA2 were markedly overexpressed in DMD muscle, with fold changes of 8.0 and 7.8, respectively (**Figure 3B**). These findings are consistent with previous reports of ANXA1 and ANXA2 upregulation in DMD patient cohorts and in mdx mice [4,11], and confirm their dysregulation in human DMD muscle. In summary, while ANXA5 and ANXA6 expression is minimally altered, ANXA1 and ANXA2 are strongly upregulated in DMD skeletal muscle tissue. To extend our analysis, we examined annexin expression in myotubes derived from control and DMD patient cell lines differentiated for three days (**Figure 4A**). ANXA5 and ANXA6 were detected as single bands at their expected molecular weights of 35 kDa and 68 kDa, respectively. In contrast, ANXA1 and ANXA2 appeared as multiple bands - up to three - likely reflecting

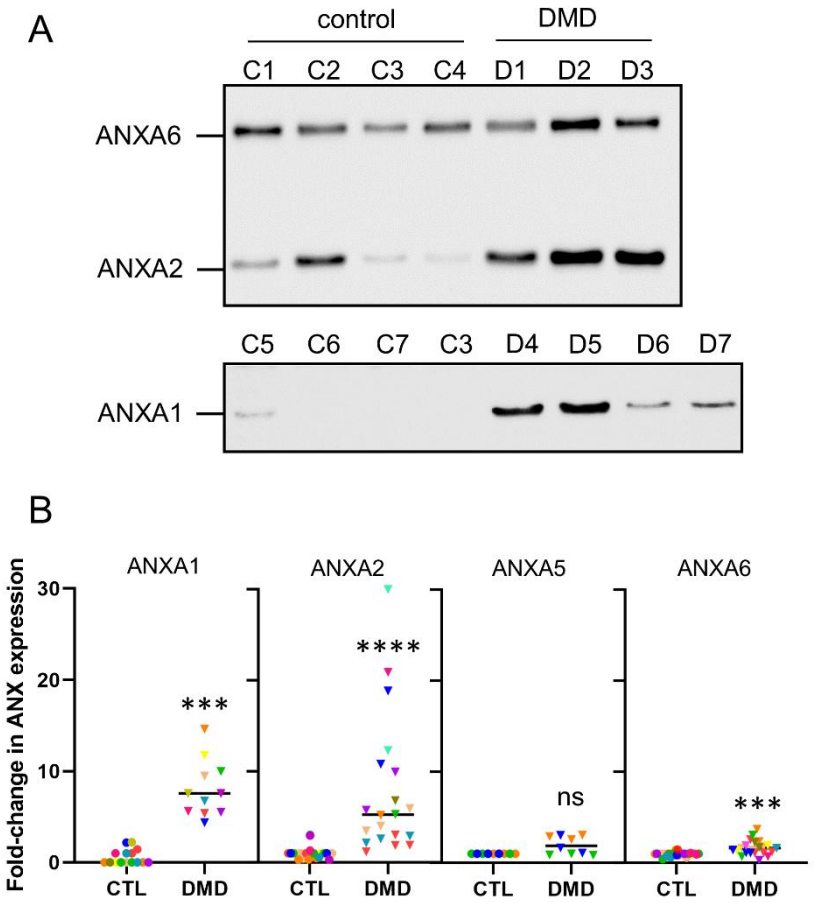

FIGURE 3 Annexin expression in control and DMD skeletal muscle biopsies. A) Annexin expression was quantified by western-blot analysis. Normalization was performed by total protein detection. Full membranes are presented in supplementary Figure S3. B) Annexin expression quantified by western-blot analysis from biopsies of control individuals (n = 7) or DMD patients (n = 7). Wilcoxon signed rank test. ***: $p < 0.001$; ****: $p < 0.0001$.

known post-translational modifications, including proteolytic cleavage and phosphorylation [25–28]. To quantify overall protein abundance, all bands corresponding to a given annexin were summed, and data from the two control and two DMD cell lines were pooled to improve statistical robustness (**Figure 4B**). No significant differences were observed in ANXA5 or ANXA6 expression between control and DMD myotubes. A modest increase in ANXA1 expression was noted in DMD cells, although this difference was primarily driven by a single pairwise comparison (DMD2 vs. CTL1; **Figure S5**) and was not consistent across all samples. By contrast, ANXA2 expression was significantly elevated in DMD myotubes, with an average increase of approximately 30% relative to control (**Figure 4B; Figure S5**). These data confirm that ANXA2 is selectively upregulated in DMD muscle cells in vitro, while levels of ANXA1, ANXA5, and ANXA6 remain largely unchanged.

We hypothesized that the lack of ANXA1 upregulation in DMD myotubes might be due to the absence of mechanical stimulation, which is prevalent in vivo. To test this, we analyzed the expression of annexins in 24-hour-differentiated myoblasts exposed or not to shear stress. This approach was guided by two hypotheses: (1) mechanical stimulation enhances the membrane repair machinery in healthy muscle cells as an adaptive response to future sarcolemmal damage, and (2) this adaptive mechanism is impaired in dystrophic cells. Supporting the first hypothesis, previous studies have shown that annexin expression is upregulated in invasive cancer cells subjected to intense mechanical stress [29–31].

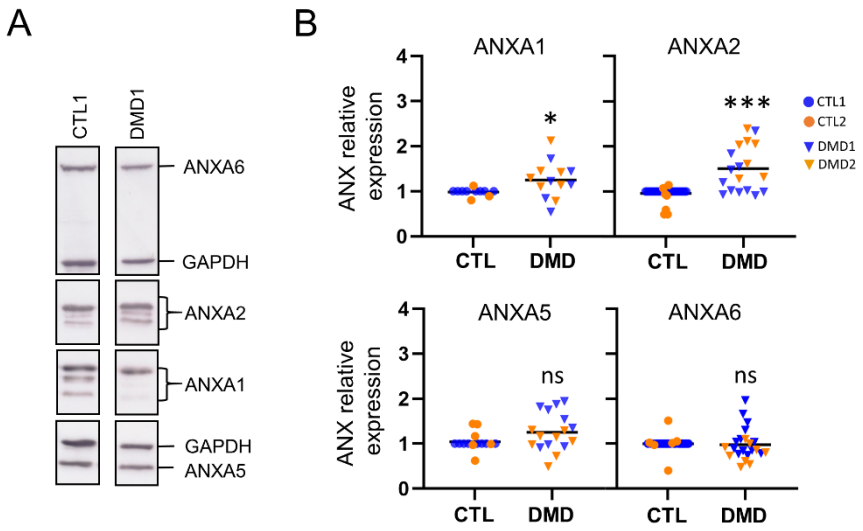

FIGURE 4 Annexin expression in control and DMD skeletal muscle cell lines. A) Annexin expression was quantified by western-blot analysis from myotubes. Each sample was systematically analyzed on four independent membranes for detecting ANXA1, ANXA2, ANXA5 or ANXA6. As ANXA1 and ANXA2 molecular weight is similar to GAPDH, this loading control was immunodetected only on ANXA5 and ANXA6 membranes. The full membranes are presented in supplementary Figure S4. B) Data were systematically normalized with GAPDH and CTL1 was used as an internal control. Wilcoxon signed rank test using CTL1 as a reference. *: $p < 0.05$; ***: $p < 0.001$.

We quantified ANXA1, ANXA2, ANXA5, and ANXA6 levels in control and DMD cell lines 24 hours after shear stress and compared them to untreated counterparts (**Figure 5**). In control cells, shear stress induced an increase of about 20% in ANXA5 and ANXA6 expression, whereas ANXA1 and ANXA2 levels remained unchanged (**Figure 5B**). These findings suggest that mechanical stress selectively enhances the expression of ANXA5 and ANXA6, potentially reinforcing membrane repair capacity. In contrast, DMD cells failed to upregulate ANXA5 and ANXA6 in response to shear stress, indicating a blunted adaptive response. We conclude that DMD muscle cells exhibit an impaired ability to modulate key membrane repair components under mechanical challenge. Together, our findings demonstrate that ANXA1 and ANXA2 are overexpressed in muscle biopsies from DMD patients. This upregulation was confirmed in cultured skeletal muscle cells for ANXA2, but not for ANXA1. Furthermore, we showed that mechanical stress induces a significant increase in ANXA5 and ANXA6 expression in myotubes derived from control individuals, suggesting that healthy muscle cells can enhance their membrane repair machinery in anticipation of future sarcolemmal injury.

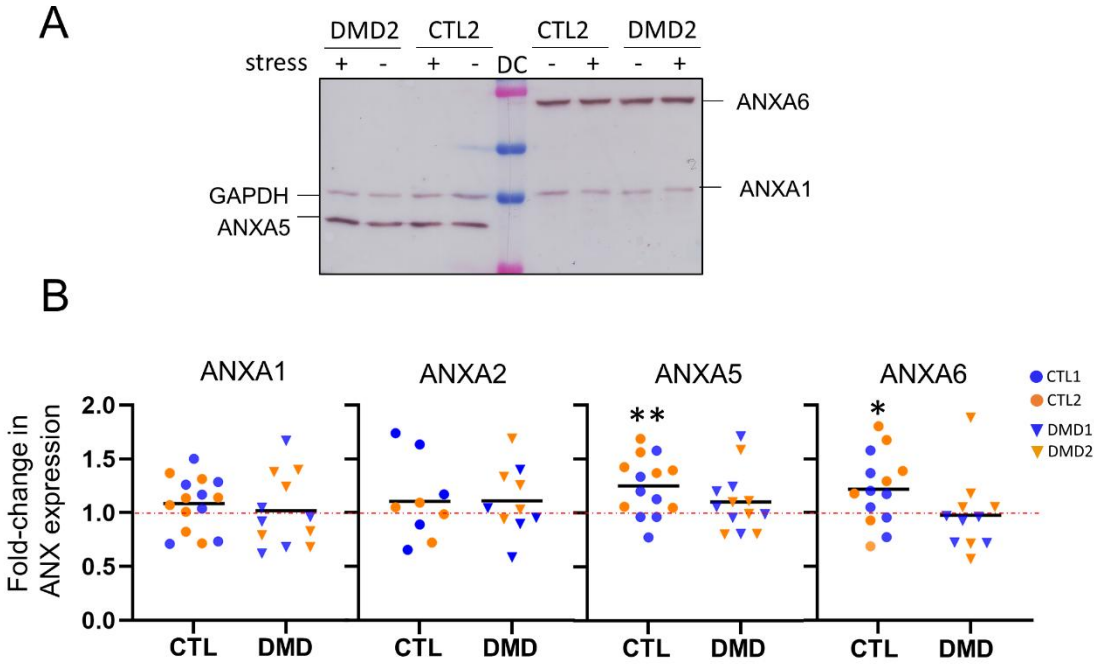

FIGURE 5 Annexin expression in control and DMD skeletal muscle submitted to shear stress. A) Example of western blot analyzing the expression of ANXA1, ANXA2, ANXA5, and ANXA6 in CTL2 and DMD2 cell lines submitted (+) or not (-) to shear stress. The Dual color molecular weight marker (DC, Biorad) has been used. The entire membrane is presented in Figure S6A. B) Scatter plot with mean value displaying the fold-change of annexin expression in control and DMD skeletal muscle cell lines after shear stress normalized for the basal unstressed condition. The dashed red line the baseline corresponding to the absence of annexin expression after shear stress. Wilcoxon test. *: $p < 0.05$; **: $p < 0.01$. Data obtained on each cell line are presented in Figure S6B.

Notably, this adaptive response was absent in DMD cells, which failed to upregulate ANXA5 and ANXA6 under mechanical stress, indicating a compromised ability to modulate their repair capacity in response to environmental challenges.

3.3. Histological Distribution of Annexins is Disturbed in DMD Muscle

We next examined the localization of annexins in control and DMD muscle biopsies using immunohistofluorescence. In control samples, ANXA1 and ANXA2 were weakly and diffusely distributed within the cytoplasm of myofibers (**Figure 6**). Additionally, ANXA2 was detected at the sarcolemma and within endothelial cells (**Figure 6,** white arrows). In contrast, DMD biopsies showed increased extracellular localization of ANXA1 and, more markedly, ANXA2, suggesting leakage from damaged myofibers (**Figure 6**). For ANXA5, we observed expression in only a subset of myofibers, where it was predominantly cytoplasmic (**Figure 6**). Co-immunostaining with fast myosin heavy chain revealed that ANXA5 expression was restricted to type II myofibers (**Figure S7A**). We found that the proportion of ANXA5-positive myofibers was reduced to approximately 25% in DMD biopsies (**Figure S7B**). In control samples, ANXA6 was localized both in the cytoplasm and at the sarcolemma of muscle fibers (**Figure 6**). In DMD biopsies, ANXA6 was observed to accumulate at the sarcolemma in some myofibers, likely reflecting a response to membrane damage (**Figure 6**, white asterisks). Taken together, these findings indicate that DMD myofibers - predominantly type I - experience extensive sarcolemmal damage, associated with defective membrane repair mechanisms and the abnormal presence of annexins, particularly ANXA2, in the extracellular space. To further investigate whether

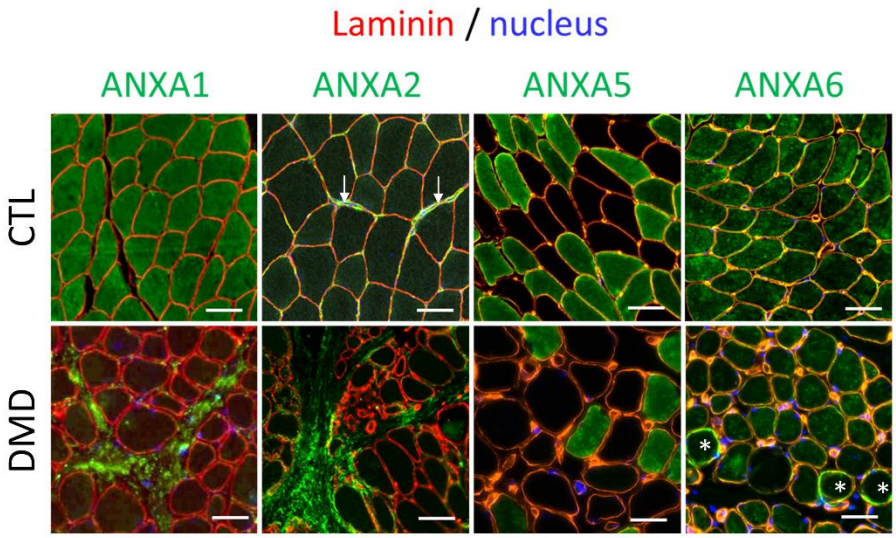

FIGURE 6 Analysis of annexin distribution in control and DMD biopsies. Distribution of annexin in control (n=3) and DMD (n=3) biopsies was analyzed by immunohistofluorescence. Laminin-α (red) was also immunostained to detect sarcolemma. White arrows point out the presence of ANXA2 in the sarcolemma. White asterisks indicate myofibers where ANXA6 concentrated within the sarcolemma. Scale bar = 50 µm.

ANXA2 is released from damaged and unrepaired DMD muscle cells, we analyzed the dynamics of GFP-tagged ANXA2 in laser-injured human skeletal muscle cells. In control cells, ANXA2-GFP was rapidly recruited to the sarcoplasmic side of the injury site, where it remained concentrated for several minutes (**Figure 7A–B**), consistent with its role in lipid patch formation, as previously described

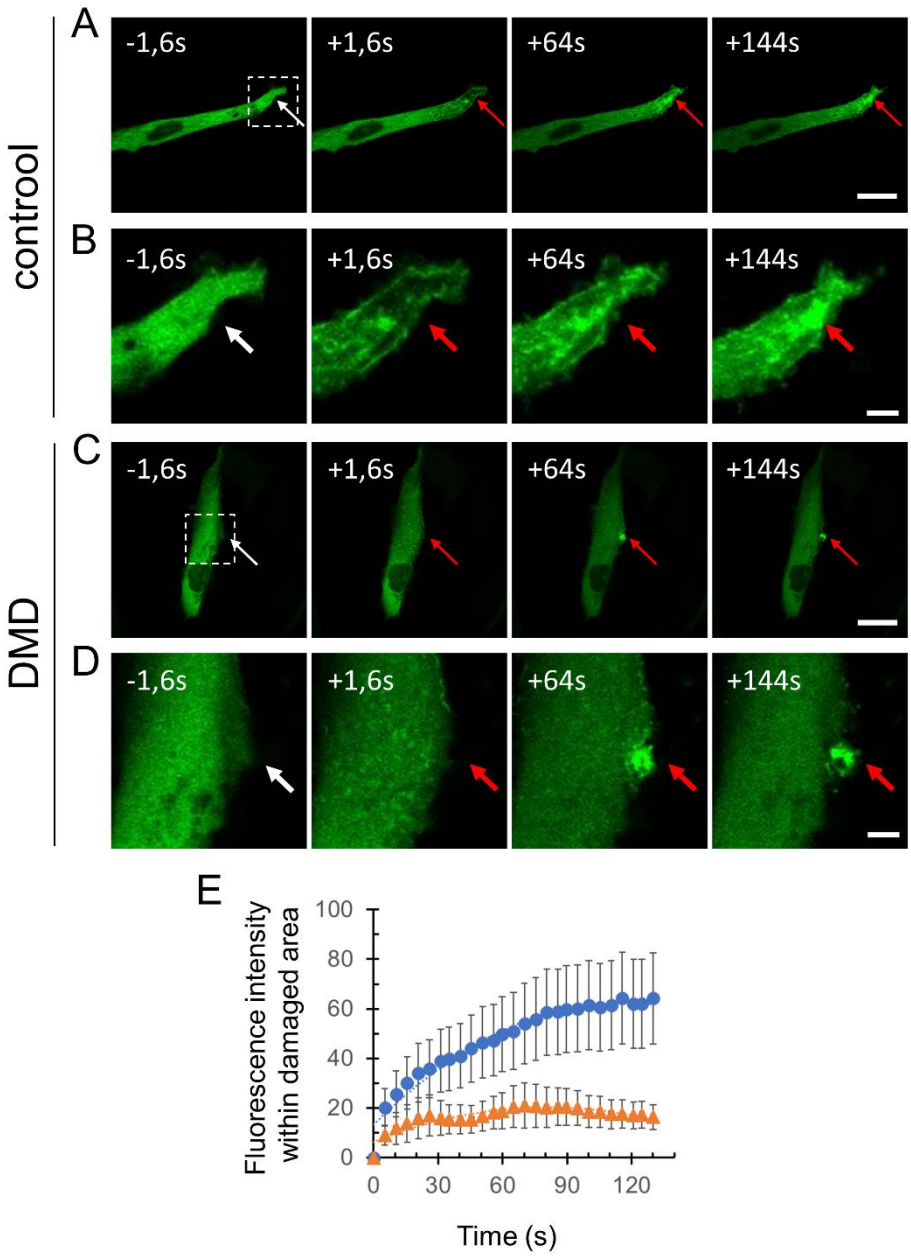

FIGURE 7 Trafficking of ANXA2 in control or DMD skeletal muscle cells damaged by laser ablation. A-B) ANXA2 expressing CTL1 myoblasts were damaged by laser ablation. In B, magnified images of the area framed (dotted line) in A. C-D) ANXA2 expressing DMD1 myoblasts were damaged by laser ablation. In D, magnified images of the area framed (dotted line) in C. White arrow, area before irradiation; red arrow, area after irradiation. Scale bar for images A and C: 15 µm, B and D: 2.5 µm. E) Traffic of ANXA2 at the disruption site. Data (mean ± SD) represent the ANXA2-GFP fluorescence intensity integrated over a 10 µm-diameter ROI, which is plotted versus time. Circular ROI was drawn from the damaged site toward the cytoplasm. For CTL and DMD myoblasts, n = 6.

(Lennon et al. 2003; Croissant et al. 2022). While ANXA2 also localized to damage sites in DMD cells (**Figure 7C–D**), the fluorescence intensity at these sites remained significantly lower than in controls (**Figure 7E**). Since the overall intracellular trafficking of ANXA2 appeared similar between control and DMD cells (**Figure S8**), the reduced signal observed at the lesion likely reflects extracellular leakage of ANXA2 from DMD myofibers, supporting the hypothesis of compromised membrane resealing.

3.4. Adipocyte Accumulation in DMD Biopsies

In LGMD2B, the presence of extracellular ANXA2 has been linked to enhanced muscle adipogenesis, partly through its influence onto FAPs [3]. To explore whether a similar process may contribute to disease progression in Duchenne muscular dystrophy (DMD), we analyzed the localization of perilipin, a lipid droplet-associated protein and marker of adipocytes, in skeletal muscle biopsies from control individuals and DMD patients. While perilipin staining was undetectable in control samples, DMD biopsies displayed extensive perilipin-positive areas, reflecting significant adipogenic infiltration (**Figure 8**). These findings suggest that chronic membrane disruption and defective repair in DMD muscle fibers promote the release of cytosolic factors such as ANXA2 into the extracellular space, which may in turn drive adipogenic conversion of FAPs. This mechanism, previously described in LGMD2B [3], may thus be a common feature of muscular dystrophies characterized by defective membrane repair, contributing to fatty degeneration of muscle tissue and functional decline.

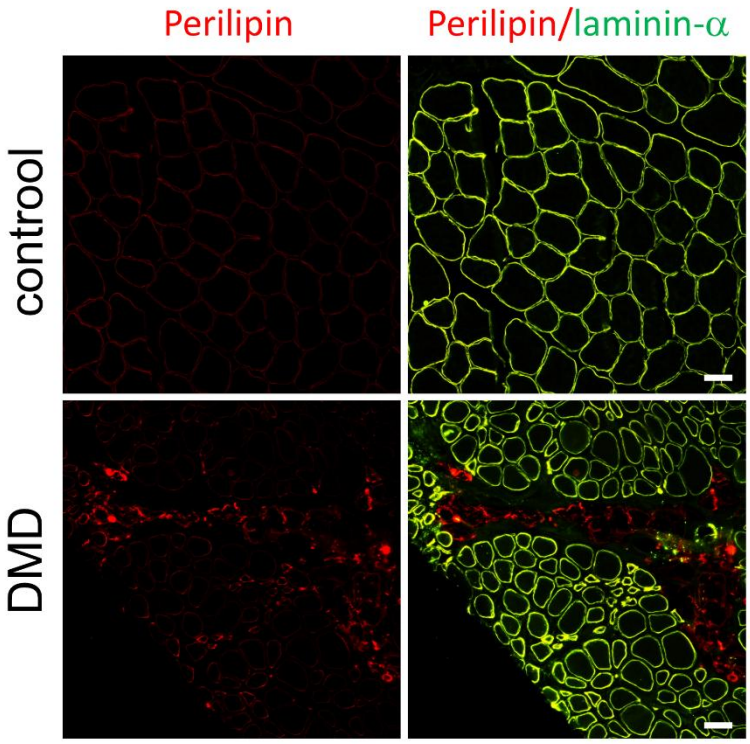

FIGURE 8 Analysis of perilipin distribution in control and DMD biopsies. Distribution of perilipin (red) in control (n=3) and DMD (n=3) biopsies was analyzed by immunohistofluorescence. Laminin-α (green) was also immunostained to detect sarcolemma. Scale bar = 50 µm.

4. Discussion

Here, we demonstrated that human DMD muscle cells are intrinsically defective in membrane repair, a critical function for maintaining muscle integrity during mechanical stress. Using a combination of histological, functional, and molecular analyses, we established that the sarcolemma fragility and the inability to effectively repair membrane lesions are key contributors to muscle cell death, adipogenesis, and progressive muscle loss in DMD. Through immunostaining of patient muscle biopsies, we confirmed that DMD muscle fibers frequently exhibit sarcolemmal injuries, as evidenced by the widespread intracellular presence of IgG, which was absent in control tissues. This observation is consistent with previous studies showing that dystrophin deficiency destabilizes the sarcolemma and severely compromises the mechanical stability of muscle fibers, making them highly susceptible to injury [8,32]. To specifically assess membrane repair capacity, we employed a recently developed muscle shear stress assay [17]. DMD muscle cells exhibited a significantly higher proportion of damaged and unrepaired cells compared to controls, reaching levels similar to those seen in LGMD2B, a known membrane repair-deficient disease [2]. Crucially, the shear stress experiments in Ca^{2+}-free conditions showed no difference in intrinsic membrane fragility between DMD and control cells, confirming that the defect lies in the repair process itself rather than in increased mechanical vulnerability. Jaiswal and collaborators previously emphasized the role of mitochondria in membrane repair and identified mitochondrial dysfunction as a key contributor to DMD pathology in the mdx mouse model [11]. In dystrophin-deficient murine muscle fibers, mitochondrial dynamics and function were compromised, leading to ineffective repair and increased myofiber death. A comparable mechanism is likely at play in human DMD. Together, these findings firmly establish that, similar to LGMD2B, the fundamental defect in human DMD resides in defective membrane repair of skeletal muscle cells.

At the molecular level, we found that annexin expression is dysregulated in DMD muscle. In biopsies, ANXA1 and ANXA2 were significantly overexpressed, while ANXA5 and ANXA6 showed only modest changes. This aligns with previous findings in both human DMD samples [4] and mdx mice [11]. Under cell culture conditions, only ANXA2 was consistently overexpressed in DMD myotubes, while ANXA1 levels remained similar between DMD and control cells. Suspecting that the absence of mechanical stress in vitro might explain this observation, we examined the impact of mechanical stress on sarcoplasmic annexin expression. We found that mechanical stress promoted the upregulation of ANXA5 and ANXA6 in control cells, whereas DMD cells failed to adjust their annexin expression in response to stress. These findings suggest that DMD muscle cells are impaired not only in membrane repair but also in their capacity to adapt to mechanical stress. Immunofluorescence analyses further revealed that the subcellular distribution of annexins is disrupted in DMD muscle. While ANXA1 and ANXA2 were

diffusely cytoplasmic in controls, they were observed in the extracellular milieu in DMD samples, suggesting that membrane lesions allow annexin leakage. Interestingly, ANXA2 was particularly abundant outside myofibers in DMD tissue. Consequently, defects in membrane repair not only lead to direct myofiber degeneration but also initiate secondary pathological cascades involving the muscle environment. In this regard, it has been reported that in LGMD2B, persistent membrane damage promotes the activation and pathological differentiation of FAPs, contributing significantly to fatty infiltration and muscle loss [3]. A similar mechanism may occur in DMD, where defective membrane repair could lead to abnormal activation of FAPs, promoting adipocyte accumulation and worsening muscle degeneration. A previous work has indeed reported a significant expansion of the FAP population in muscle biopsies from DMD patients compared to healthy controls [33]. To further investigate this hypothesis, we performed perilipin immunohistofluorescence on control and DMD patient biopsies and found that DMD is associated with accumulation of adipocytes in the muscle interstitium. Collectively, our results establish that human DMD muscle cells have a true intrinsic defect in membrane repair. This defect is associated with abnormal annexin expression and distribution, particularly of ANXA2, and contributes to the progressive loss of muscle fibers observed in patients. Our findings highlight ANXA2 as a potential therapeutic target in DMD. Strategies that aimed at selectively inhibiting extracellular ANXA2 could offer new avenues to slow disease progression by preventing adipogenesis.

Authors Contributions

M.L.Q. performed the majority of experiments on muscle biopsies with assistance from J.R. and C.G (western-blot analysis) and S.D. (immunohistochemistry). L.A performed the majority of experiments on muscle cell lines with assistance from P.R. (western-blot analysis and shear stress assays), F.B. and A.S. (cell culture and western-blot analysis). K.M. established the AB1098 and 6594 cell lines. G.S. and M.L.M.N. were responsible for the establishment and long-term management of the biobank providing human muscle biopsies. A.B. coordinated the entire project and designed the experiments. A.B. wrote the manuscript with the help of M.L.M.N. and M.L.Q.

Funding

This research was funded by AFM-telethon (grant 22442 to A.B., grant 24991 to A.B. and M.L.M.N. and grant 23881 to L.A.).

Acknowledgments

The authors acknowledge the AFM-telethon association for its financial support (Grant 23881 to L.A. and 22442 and 24991 to A.B. and M-L.M-N). The authors thank the Centre de Ressources Biologiques

Plurithematique of the Bordeaux University Hospital (BB-0033-00094) for providing the material used in this research. We are also deeply grateful to the COLMYONEU muscle bank donors for their generous donation of the tissue samples used in this study. The HistoCARE facility of IMN (UMR5293, unit of the CNRS and Bordeaux University) is acknowledged for performing part of the IHC experiments. The authors wish to acknowledge MyoLine, the platform for the immortalization of human cells from the Institute of Myology in Paris for the establishment of muscle cell lines. Christel Poujol and Sébastien Marais are acknowledged for the help in studies of trafficking of ANXA2 that were done in the Bordeaux Imaging Center a service unit of the CNRS-INSERM and Bordeaux University, member of the national infrastructure France BioImaging supported by the French National Research Agency (ANR-10-INBS-04).

Ethic statement

This study has been approved by the appropriate ethics committee and has therefore been performed in accordance with the ethical standards laid down in the 1964 Declaration of Helsinki and its later amendments. All patients gave their informed consent prior to their inclusion in the study.

Conflicts of interest

The authors declare no conflicts of interest.

Bibliography

1. McNeil PL, Steinhardt RA. Plasma membrane disruption: repair, prevention, adaptation. *Annu Rev Cell Dev Biol* 2003;**19**:697–731.

2. Bansal D, Miyake K, Vogel SS, Groh S, Chen C-C, Williamson R *et al.* Defective membrane repair in dysferlin-deficient muscular dystrophy. *Nature* 2003;**423**:168–172.

3. Hogarth MW, Defour A, Lazarski C, Gallardo E, Manera JD, Partridge TA *et al.* Fibroadipogenic progenitors are responsible for muscle loss in limb girdle muscular dystrophy 2B. *Nat Commun* 2019;**10**.

4. Cagliani R, Magri F, Toscano A, Merlini L, Fortunato F, Lamperti C *et al.* Mutation finding in patients with dysferlin deficiency and role of the dysferlin interacting proteins annexin A1 and A2 in muscular dystrophies. *Hum Mutat* 2005;**26**:283.

5. Novak ML, Weinheimer-Haus EM, Koh TJ. Macrophage activation and skeletal muscle healing following traumatic injury. *Journal of Pathology* 2014;**232**:344–355.

6. Hoffman EP, Brown RH, Kunkel LM. Dystrophin: the protein product of the Duchenne muscular dystrophy locus. *Cell* 1987;**51**:919–928.

7. Ervasti JM, Campbell KP. Membrane organization of the dystrophin-glycoprotein complex. *Cell* 1991;**66**:1121–1131.

8. Petrof BJ, Shrager JB, Stedman HH, Kelly AM, Sweeney HL. Dystrophin protects the sarcolemma from stresses developed during muscle contraction. *Proc Natl Acad Sci U S A* 1993;**90**:3710–3714.

9. Wallace GQ, McNally EM. Mechanisms of muscle degeneration, regeneration, and repair in the muscular dystrophies. *Annu Rev Physiol* 2009;**71**:37–57.

10. Jungbluth H, Treves S, Zorzato F, Sarkozy A, Ochala J, Sewry C *et al.* Congenital myopathies: disorders of excitation-contraction coupling and muscle contraction. *Nat Rev Neurol* 2018;**14**:151–167.

11. Vila MC, Rayavarapu S, Hogarth MW, Van der Meulen JH, Horn A, Defour A *et al.* Mitochondria mediate cell membrane repair and contribute to Duchenne muscular dystrophy. *Cell Death Differ* 2017;**24**:330–342.

12. Collins CA, Morgan JE. Duchenne's muscular dystrophy: animal models used to investigate pathogenesis and develop therapeutic strategies. *Int J Exp Pathol* 2003;**84**:165–172.

13. Mamchaoui K, Trollet C, Bigot A, Negroni E, Chaouch S, Wolff A *et al.* Immortalized pathological human myoblasts: towards a universal tool for the study of neuromuscular disorders. *Skelet Muscle* 2011;**1**:34.

14. Echigoya Y, Lim KRQ, Melo D, Bao B, Trieu N, Mizobe Y *et al.* Exons 45-55 Skipping Using Mutation-Tailored Cocktails of Antisense Morpholinos in the DMD Gene. *Mol Ther* 2019;**27**:2005–2017.

15. Tasca F, Brescia M, Liu J, Janssen JM, Mamchaoui K, Gonçalves MAFV. High-capacity adenovector delivery of forced CRISPR-Cas9 heterodimers fosters precise chromosomal deletions in human cells. *Mol Ther Nucleic Acids* 2023;**31**:746–762.

16. Carmeille R, Bouvet F, Tan S, Croissant C, Gounou C, Mamchaoui K *et al.* Membrane repair of human skeletal muscle cells requires Annexin-A5. *Biochim Biophys Acta Mol Cell Res* 2016;**1863**:2267–2279.

17. d'Agata L, Rassinoux P, Gounou C, Bouvet F, Bouragba D, Mamchaoui K *et al.* A Novel Assay Reveals the Early Setting-Up of Membrane Repair Machinery in Human Skeletal Muscle Cells. *J Cell Biochem* 2024;**126**:e30.

18. Croissant C, Gounou C, Bouvet F, Tan S, Bouter A. Trafficking of Annexins during Membrane Repair in Human Skeletal Muscle Cells. *Membranes 2022, Vol 12, Page 153* 2022;**12**:153.

19. Bencze M, Periou B, Baba-Amer Y, Authier FJ. Immunolabelling Myofiber Degeneration in Muscle Biopsies. *J Vis Exp* 2019;**2019**.

20. Heydemann A, Huber JM, Demonbreun A, Hadhazy M, McNally EM. Genetic background influences muscular dystrophy. *Neuromuscular Disorders* 2005;**15**:601–609.

21. Quattrocelli M, Capote J, Ohiri JC, Warner JL, Vo AH, Earley JU *et al.* Genetic modifiers of muscular dystrophy act on sarcolemmal resealing and recovery from injury. *PLoS Genet* 2017;**13**:e1007070.

22. Vilchez JJ, Gallano P, Gallardo E, Lasa A, Rojas-García R, Freixas A *et al.* Identification of a novel founder mutation in the DYSF gene causing clinical variability in the spanish population. *Arch Neurol* 2005;**62**:1256–1259.

23. Swaggart KA, Demonbreun AR, Vo AH, Swanson KE, Kim EY, Fahrenbach JP *et al.* Annexin A6 modifies muscular dystrophy by mediating sarcolemmal repair. *Proc Natl Acad Sci U S A* 2014;**111**:6004–6009.

24. Demonbreun AR, Allen M V, Warner JL, Barefield DY, Krishnan S, Swanson KE *et al.* Enhanced Muscular Dystrophy from Loss of Dysferlin Is Accompanied by Impaired Annexin A6 Translocation after Sarcolemmal Disruption. 2016;**186**:1610–1622.

25. Babiychuk EB, Monastyrskaya K, Burkhard FC, Wray S, Draeger A. Modulating signaling events in smooth muscle: cleavage of annexin 2 abolishes its binding to lipid rafts. *The FASEB Journal* 2002;**16**:1177–1184.

26. Wang CY, Lin CF. Annexin A2: Its molecular regulation and cellular expression in cancer development. *Dis Markers* 2014;**2014**.

27. Grindheim AK, Saraste J, Vedeler A. Protein phosphorylation and its role in the regulation of Annexin A2 function. Biochim Biophys Acta Gen Subj. 2017;**1861**:2515–2529.

28. Gabel M, Delavoie F, Royer C, Tahouly T, Gasman S, Bader MF *et al.* Phosphorylation cycling of Annexin A2 Tyr23 is critical for calcium-regulated exocytosis in neuroendocrine cells. *Biochim Biophys Acta Mol Cell Res* 2019;**1866**:1207–1217.

29. Bouvet F, Ros M, Bonedeau E, Croissant C, Frelin L, Saltel F *et al.* Defective membrane repair machinery impairs survival of invasive cancer cells. *Sci Rep* 2020;**10**:21821.

30. Gounou C, Bouvet F, Liet B, Prouzet-Mauléon V, D'Agata L, Harté E *et al.* Annexin-A5 and annexin-A6 silencing prevents metastasis of breast cancer cells in zebrafish. *Biol Cell* 2023;**115**:e202200110.

31. Gounou C, Rouyer L, Siegfried G, Harté E, Bouvet F, d'Agata L *et al.* Inhibition of the membrane repair protein annexin-A2 prevents tumor invasion and metastasis. *Cellular and Molecular Life Sciences* 2024;**81**:1–16.

32. Carmignac V, Durbeej M. Cell-matrix interactions in muscle disease. *J Pathol* 2012;**226**:200–218.

33. Cardone N, Taglietti V, Baratto S, Kefi K, Periou B, Gitiaux C *et al.* Myopathologic trajectory in Duchenne muscular dystrophy (DMD) reveals lack of regeneration due to senescence in satellite cells. *Acta Neuropathol Commun* 2023;**11**.